ACS OMEGA

http://pubs.acs.org/journal/acsodf

Article

Quantification of a Neurological Protein in a Single Cell Without Amplification

Donggyu Lee, Youngsik Woo, Ji-seon Lim, Ikbum Park, Sang Ki Park,* and Joon Won Park*

Cite This: *ACS Omega* 2022, 7, 20165−20171

Read Online

ACCESS | Metrics & More | Article Recommendations | Supporting Information

ABSTRACT: Proteins are key biomolecules that not only play various roles in the living body but also are used as biomarkers. If these proteins can be quantified at the level of a single cell, understanding the role of proteins will be deepened and diagnosing diseases and abnormality will be further upgraded. In this study, we quantified a neurological protein in a single cell using atomic force microscopy (AFM). After capturing specifically disrupted-in-schizophrenia 1 (DISC1) in a single cell onto a microspot immobilizing the corresponding antibody on the surface, force mapping with AFM was followed to visualize individual DISC1. Although a large variation of the number of DISC1 in a cell was observed, the average number is 4.38×10^3, and the number agrees with the ensemble-averaged value. The current AFM approach for the quantitative analysis of proteins in a single cell should be useful to study molecular behavior of proteins in depth and to follow physiological change of individual cells in response to external stimuli.

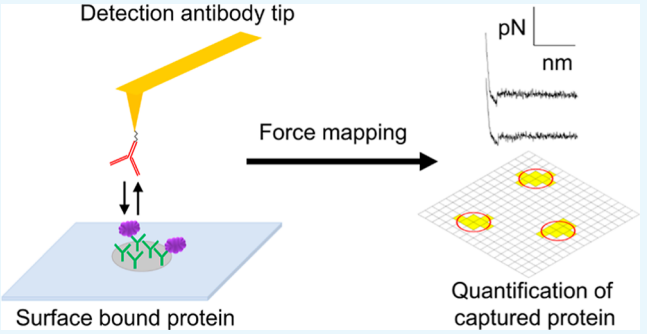

INTRODUCTION

Proteins are utmost important to biological processes, providing structural supports, transporting molecules, controlling cell growth and adhesion, regulating cell signaling, and catalyzing biochemical reactions.[1,2] Therefore, accurate protein quantification is essential for studying cellular mechanisms, elaborating diagnostics, and pursuing drug discovery and developments.[3] A lot of methods and tools have been developed, and examples are gel electrophoresis, immunoassay, chromatography, and mass spectrometry.[4−6] However, these methods require a large number of cells because of the limited sensitivity and show ensemble-averaged results.[7] For this reason, new methods enabling quantification of a specific protein in a single cell are highly desirable and anticipated.

Atomic force microscopy (AFM) has been used to study molecular interactions of ligand−receptor, DNA−DNA, and antigen−antibody at the single-molecule level.[8−20] Furthermore, AFM force mapping can show the target molecule distribution on a sample surface by recording the force−distance (FD) curve at a high resolution.[21] Recently, we demonstrated that such AFM analysis quantifies specific DNA and miRNA of a low copy number without labeling or amplification.[22−24]

In this study, we employed force-based AFM to quantify a specific protein in a single cell. Previously, Roy et al.[25] visualized prostate-specific antigen captured on the surface, and because they utilized a conventional microarrayer to generate the capture spot, the observed limit of detection (LOD) was a few femtomoles of concentration. In order to enhance LOD that is good for the single-cell analysis, we adopted the FluidFM technology to fabricate capture antibody spots of a few micrometers in diameter, and the combined approach was able to quantify the target protein in a single cell.[26]

The target protein is disrupted-in-schizophrenia 1 (DISC1), and it is a major susceptibility factor for schizophrenia. It was first identified as a gene disrupted by the translocation in chromosome 1 and discovered from a pedigree in which many family members suffered from major psychosis.[27] DISC1 participates in neuro-developmental processes including neurogenesis, neuronal migration, neurite outgrowth, dendritic spine maturation, and adult neurogenesis,[28−36] and it regulates microtubule-based motor activities, cAMP signaling, transcription factor activities, and mitochondrial functionalities.[37−44]

RESULTS

Capture Antibody Spot Fabrication and AFM Force Mapping of Captured DISC1. The FluidFM technology was used to fabricate capture antibody spots, in which a

Received: April 1, 2022
Accepted: May 25, 2022
Published: June 2, 2022

https://doi.org/10.1021/acsomega.2c02009
ACS Omega 2022, 7, 20165−20171

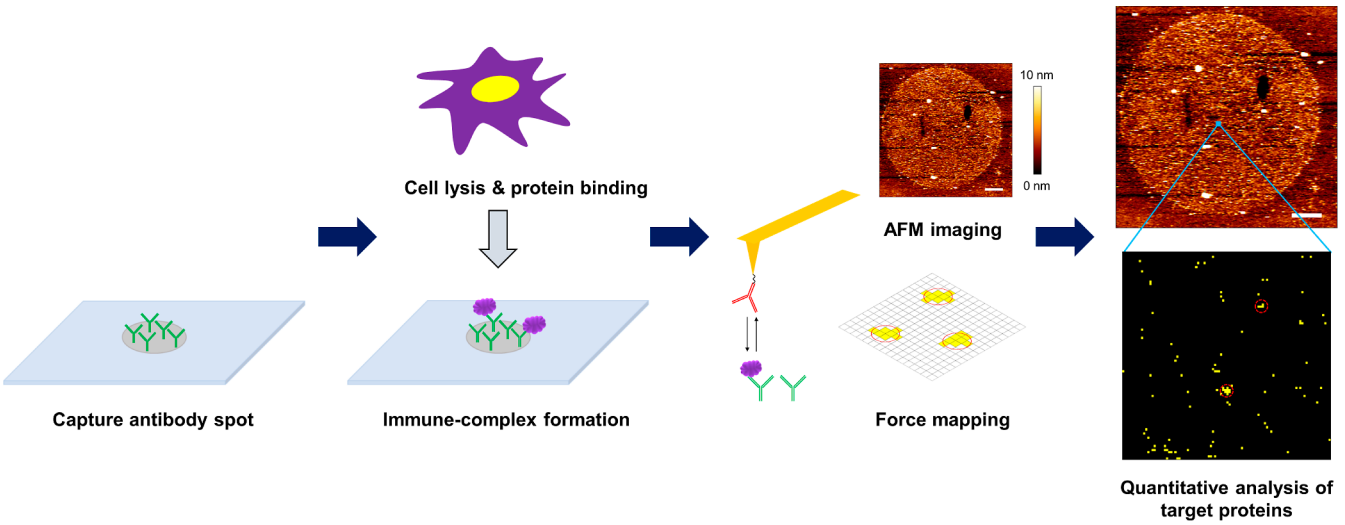

Figure 1. Experimental scheme for the analysis of DISC1 protein with AFM. For the quantification of DISC1 protein, a single cell was lysed and DISC1 proteins were bound to a capture antibody spot. The capture antibody/DISC1 immune complex was detected by observing specific force–distance curves upon the approach and retraction of the detection antibody tip. Bound DISC1 proteins show themselves as clusters on the adhesion force map. Scale bar, 2.0 μm.

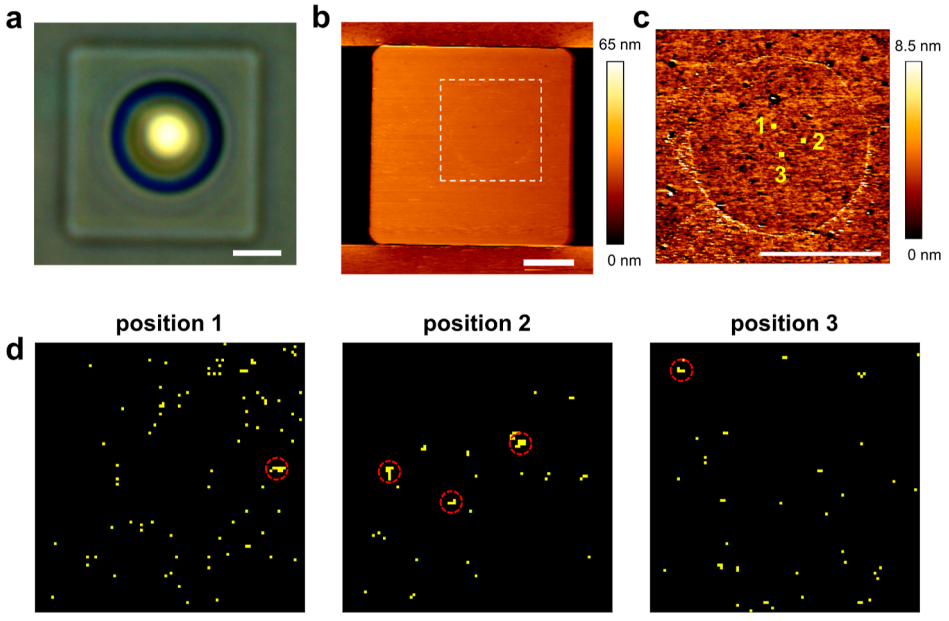

Figure 2. AFM image of a capture spot and representative force maps. (a) Optical microscopy image of a capture antibody spot. Scale bar, 5.0 μm. (b) AFM height image of the etched square box. Scale bar, 5.0 μm. (c) AFM height image of a capture antibody spot. Numbered small squares are the areas where AFM force mapping was performed. Scale bar, 5.0 μm. (d) Force maps of three colored positions in the immune complex spot. Colored pixels show that specific unbinding events were observed more than twice out of five measurements (100 × 100 pixels, 400 × 400 nm^2). Five qualified clusters in the maps are evident.

microchanneled cantilever equipped with a pyramidal tip of 600 nm aperture was employed.[26] The microchannel was filled with the capture antibody solution, and the solution was spotted onto a glass slide coated with a 27-acid dendron[45] and finally activated with *N*-hydroxysuccinimide (NHS). The typical spot diameter was in the range of 7–20 μm. To locate the antibody spot effectively for the force mapping with AFM, a glass slide marked by multiple micron-sized square boxes through the photolithographic etching was used (Figure S1), and positional coordinates of the spot were recorded after the spotting.

After allowing DISC1 to be captured on the spot, thus-formed immune complexes were chemically cross-linked to avoid sporadic detachment during AFM examination.[46] FD curves were collected on the capture spot at a resolution of 3.0 or 4.0 nm, and the specific unbinding events were recorded when the detection antibody on the AFM tip binds with DISC1/capture antibody immune complexes (Figure 1). The selected detection antibody binds to an epitope free after the formation of the immune complex in the capture spot. The FD curves were recorded five times at each pixel at 3.0 nm intervals across a selected area (60 nm × 60 nm) and marked only when no less than 40% specific FD curves were observed

https://doi.org/10.1021/acsomega.2c02009
ACS Omega 2022, 7, 20165–20171

(in other words, two times out of five measurements). Gaussian fitting shows the most probable adhesion force of 44.0 ± 12.8 pN and the stretching distance of 7.6 ± 2.6 nm (Figure S2). The adhesion force value is similar to the ones observed from other antigen−antibody pairs.[15]

The cluster radius (R_c) was measured by ellipse fitting to identify the hydrodynamic radius of the target protein.[47] Three clusters were identified from three different locations, and the average cluster radius was 7.8 ± 0.4 nm (Figure S3). Based on the value, we were able to determine the optimized pixel size (4 nm) in which DISC1 shows itself as a cluster in the force map (with a too large pixel, the scanning is speedy but may miss DISC1 on the surface, and with a too small pixel, DISC1 will show up as an evident cluster, but the time efficiency is deteriorated). Therefore, we examined the selected area (400 nm × 400 nm) at each 4 nm (100 × 100 pixels). We counted clusters at three representative locations in a spot and calculated the total number of the bound protein in the entire spot by assuming uniform distribution and homogeneity.

As a control, NDEL1 (another neurological protein exists in the same cell) was allowed to the surface and FD curves were collected. Because the specific FD curve was not observed at all (Figure S4), it is confirmed that the current AFM analysis is specific to DISC1.

Quantitative Analysis of DISC1 Protein in a Single Cell. As a first step, DISC1 proteins obtained from lysed HEK293 cells were analyzed. We prepared 4×10^5 sorted cells through the cell culture, and fractionation, lysis, and serial dilution made lysed samples corresponding to 10 cells. Each sample was allowed to react with the antibody in the spot of 20 μm. AFM force mapping was performed at three representative locations in two independently prepared immune complex spots. The observed cluster numbers were 19 and 20, and the values correspond to 3.73×10^4 and 3.93×10^4, respectively. Therefore, the average number of DISC1 in a cell was 3.83×10^3.

As the next step, we analyzed DISC1 protein in a single isolated HEK293 cell (Figure 2). Proteins extracted from the single cell were allowed to react on the antibody spots (7−14 μm). AFM force mapping was performed at three representative locations of 10 independently prepared immune complex spots. The total observed cluster numbers in the individual spots were 2, 3, 5, 7, 7, 13, 14, 15, 18, and 18. The total number of captured DISC1 in each spot was calculated by considering the size of the corresponding spot, and the numbers are 1.47×10^3, 1.79×10^3, 1.93×10^3, 1.99×10^3, 3.43×10^3, 4.97×10^3, 6.38×10^3, 6.9×10^3, 8.83×10^3, and 1.06×10^4 (Table 1, Figure 3). The mean value is 4.38 ± 3.08 × 10^3 (the standard error of the mean is 0.98 × 10^3). The value is close to the one from the diluted lysis sample (3.83×10^3). However, we observed that the copy number of each single cell varies noticeably.

For comparison, we quantified DISC1 in DISC1 knockdown HEK293 cells. A lysis sample corresponding to 10 cells and a sample of a single cell were allowed to react on antibody spots (8−11 μm). For the former, the cluster numbers were 3 and 0, and the average number of captured DISC1 was 6.65×10^2 (Table 1). It is clear that the copy number of DISC1 is reduced from 3.83×10^4 to 6.65×10^2. For the latter, because the observed cluster numbers were all 0, the number of captured DISC1 was also 0 (Table 1, Figure 3). It is interesting to observe the different outcomes for the knockdown samples. When the knockdown cells were prepared, the transfection was

Table 1. Number of DISC1 in a Single Cell or 10 Cells

	number of DISC1 in a single cell or 10 cells										
	spot 1	spot 2	spot 3	spot 4	spot 5	spot 6	spot 7	spot 8	spot 9	spot 10	mean
wild-type single cell	6.38×10^3	1.47×10^3	1.93×10^3	4.97×10^3	3.43×10^3	8.83×10^3	1.79×10^3	1.99×10^3	6.9×10^3	1.06×10^4	4.83×10^3
knockdown single cell	0	0	0								0
	spot 1	spot 2									mean
wild-type 10 cells[a]	3.73×10^4	3.93×10^4									3.83×10^4
knockdown 10 cells[a]	1.33×10^3	0									6.65×10^2

[a]The samples corresponding to 10 cells were prepared through serial dilution of the lysed solution of 4×10^5 sorted cells.

https://doi.org/10.1021/acsomega.2c02009
ACS Omega 2022, 7, 20165−20171

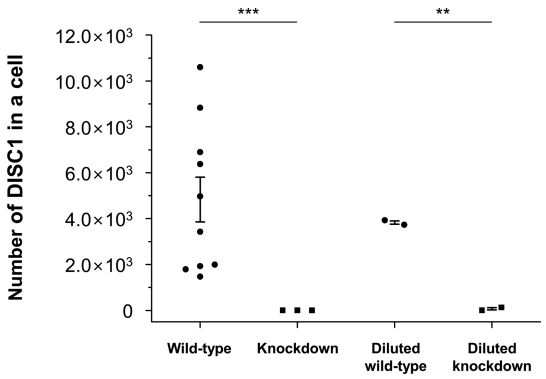

Figure 3. Number of DISC1 in a single cell. Both wild-type cells and knockdown cells were examined. The bars represent the SEM for each case (two tailed *t*-test, ***$p < 0.001$ and **$p < 0.01$).

not complete in general; it is likely that a few cells still contain DISC1. This must be the reason why we observed non-zero DISC1 in the diluted sample. However, in the case of singly isolated knockdown cells, the transfection was confirmed through use of fluorescence microscopy. As a result, AFM analysis showed that DISC1 in each single cell was 0.

DISCUSSION

We were able to quantify a specific protein in a single cell using AFM. Although various proteins exist in cells, the target DISC1 was quantified through the sandwich antibody pairs, the capture antibody on a solid substrate, and the detection antibody on an AFM tip. The specificity could be reconfirmed through the specific force−distance curves recorded during the AFM measurement.

Although the averaged number in a single cell matches with the value from the ensemble average, it is noted that the individual copy number (1.47×10^3 to 1.06×10^4) from the single cell deviates from each other considerably. While it is tempting to say that the variation represents the cell-to-cell variation and the standard error of the mean (SEM) values is low for the diluted samples, it may be too early to conclude definitely. While it is clear that the current AFM approach is sensitive enough to quantify a protein biomarker in a single cell and the approach is attractive for study of the cell-to-cell variation, re-confirmation with samples with the known variation is highly required to be accepted in the science community.

We showed previously that the LOD of a similar approach for DNA detection is a single copy. In principle, such an LOD can be realized for the protein analysis. However, it is observed that the frequency of non-specific binding is higher for the proteins. Although we isolate nucleic acids from cells or tissues and because they share the same framework (sugar and phosphate backbone), it is easier to find a condition for the specific hybridization and contingent washing by taking advantage of the well-defined melting temperature. For proteins, each sample contains polypeptides of various structures, sizes, and isoelectric points, and post-modified peptides coexist. This is the reason why we have not been able to achieve the LOD of the single copy. Although AFM itself is sensitive enough to quantify a specific protein in a single cell, we need other components to combine with AFM to increase the capability. Use of antibodies of higher specificity, surfaces providing least non-specific binding, and a right washing protocol are examples that are currently in the list. In the future, when we understand better on these topics, AFM force mapping for the quantification of protein biomarkers can move forward for further enhanced LOD.

METHODS

Conjugation of the Detection Antibody to AFM Tips. AFM tips (DPN Probe Type B, NanoInk) were coated with a 27-acid dendron (custom synthesis, VRND NanobioOrganics) as previously described.[21] For brief, silicon nitride probes were oxidized in a 10% nitric acid solution at 80 °C for 20 min. The probes were silanized in a toluene solution containing *N*-(3-(triethoxysilyl)-propyl)-*O*-poly(ethylene oxide) urethane (Gelest) [1.0% (v/v)] for 4 h. To immobilize the 27-acid dendron molecule, the silylated probes were immersed in a dimethylformamide (DMF)/dichloromethane (DCM) (1:3, v/v) solution containing the 27-acid dendron (1.0 mM), 27 mM 1,3-dicyclohexylcarbodiimide (DCC), and 0.90 mM 4-dimethylaminopyridine (DMAP) for 12 h. The dendron-modified probes were immersed in a DCM solution containing trifluoroacetic acid (1.0 M) for 12 h to remove the protecting group at the apex of the immobilized dendron. The deprotected probes were immersed in an acetonitrile solution containing bis-*N*-succinimidyl(pentaethylene glycol) ester (BS[PEG]$_5$) (25 mM) and diisopropylethylamine (DIPEA) (1.0 mM) for 4 h. After the reaction, the probes were dipped in a stirred DMF solution for 30 min, washed gently with methanol, and kept under vacuum (30−40 mTorr). The activated probes were dipped in a buffer solution [1× PBS (pH 8.5), 0.01% Tween 20, and 0.5% glycerol] dissolving the detection antibody (B-2, anti-DISC1 mouse monoclonal antibody, Santa Cruz) (33 nM) for 2 h and then washed thoroughly with PBST buffer [PBS (pH 7.4) with 0.05% Tween 20] and PBS buffer (pH 7.4) sequentially. After being washed, the probes were stored at 4 °C in PBS buffer (pH 7.4).

Fabrication of Capture Antibody Spots onto Etched Slides. Etched slides were prepared by employing inductively coupled plasma (ICP) as previously described.[18] The slides were coated with a 27-acid dendron and activated by disuccinimidyl carbonate. A microchanneled pyramidal tip of 600 nm aperture (FluidFM nanosyringe, Cytosurge AG) was employed for dispensing the detection antibody solution onto the patterned slides. The capture antibody (ABN46, anti-DISC1 rabbit polyclonal antibody, Millipore) solution (30 μM) was prepared with a spotting buffer [1× PBS (pH 8.5), 12.5% glycerol]. After injecting the solution (8 μL) into the reservoir of the FluidFM probe, it was mounted on an atomic force microscope (FlexAFM, Nanosurf) and was connected to a pressure controller (FluidFM microfluidics control system, Cytosurge AG). The cantilever was approached and contacted onto the surface, and an overpressure of +1000 mbar was applied for 30 s to fill the whole hollow cantilever. A specific set point of 200 mV was applied when the cantilever approached the sample surface. To control the droplet size, two parameters were adjusted, applied pressure and contact time of the cantilever onto the sample surface. After completion of the spotting, the slides were incubated in a humid chamber (80% humidity) at room temperature for 3 h. Subsequently, the slides were washed with PBST buffer and deionized water (18 MΩ·cm, Milli-Q purification system, Millipore). The washed slides were placed in a blocking solution containing 50 mM ethanolamine in PBS (pH 8.5) for 1 h with gentle shaking. Then, the slides were washed with PBST buffer and deionized water.

https://doi.org/10.1021/acsomega.2c02009
ACS Omega 2022, 7, 20165−20171

Antibodies and Plasmids. For developing a stable cell line to over-express hDISC1, the hDISC1 cDNA sequence was cloned into pcDNA5/TO-MYC (Invitrogen). The DISC1 shRNA construct was designed by cloning the core sequence (AAGGAAAATACTATGAAGTAC) combined with TTCAA-GAGA as the loop sequence into the pLentiLox3.7 vector as described previously.[48,49] The core sequence of control-scrambled shRNA was CTACCGTTGTATAGGTG.

Cell Culture and Transfection. HEK293 cells were cultured in DMEM (HyClone) supplemented with 10% (v/v) fetal bovine serum (FBS, Gibco) and 1% penicillin/streptomycin (Gibco). All cells were transfected by using transfection reagent Lipofectamine 2000 (Thermo Fisher Scientific).

Preparation of Cell Lysates. For 10 cell lysates, HEK293 cells or DISC1 knockdown cells were re-suspended in DMEM containing 1% FBS, followed by cell counting, and 1.0×10^4 cells were seeded in each well of a 24-well plate. After 12 h, cells were lysed in 100 μL of 1× ELB lysis buffer (50 mM Tris pH 8.0, 250 mM NaCl, 5 mM EDTA, 0.1% NP-40) supplemented with 2 mM NaPPi, 10 mM NaF, 2 mM Na_3VO_4, 1 mM DTT, and protease inhibitor cocktail (Roche) with sonication. Cell lysates were further diluted in PBS buffer (pH 7.4). For a single cell lysate, HEK293 cells or DISC1 knockdown cells were re-suspended in DMEM containing 1% FBS, diluted to 5 cells/mL, and seeded 100 μL per each well of a 96-well plate. After 12 h, each well in which a single cell exists was subjected to cell lysis with 10 μL of 1× ELB supplemented with 2 mM NaPPi, 10 mM NaF, 2 mM Na_3VO_4, 1 mM DTT, and protease inhibitor cocktail.

Formation of the Immune Complex on the Capture Antibody Spot. An eight-well gasket slide kit (Agilent Technologies) was used to incubate 40 μL of the cell lysate solution on a capture antibody-spotted slide at 25 °C for 2 h using a hybridization oven (Agilent Technologies). After the reaction, the slides were washed with a PBST solution and subsequently a PBS solution (pH 7.4). For the cross-linking, the slides were incubated with a PBS solution (pH 8.5) containing dimethyl pimelimidate−2HCl (DMP) (20 mM) at room temperature for 1 h. Subsequently, the reaction was quenched by dipping the slides in a Tris solution (20 mM, pH 7.4) for 30 min at room temperature. After the reaction, the slides were washed with a PBST solution and subsequently a PBS solution (pH 7.4), and the slides were stored at 4 °C in a PBS solution (pH 7.4).

AFM Force Measurements and Data Analysis. AFM force mapping experiments were performed using a Nano-Wizard 3 atomic force microscope (JPK Instrument). The spring constant of the AFM probes was calibrated using the thermal fluctuation method, and the measured spring constant value ranged from 0.03 to 0.04 N/m. All experiments were performed in PBS buffer (pH 7.4) at room temperature. The adhesion force map of a single target protein molecule was obtained within 60 × 60 nm^2 (20 × 20 pixels). The quantitative analysis map was obtained within 400 × 400 nm^2 (100 × 100 pixels). Five FD curves were recorded for each pixel with an approach/retraction speed of 3.0 μm/s, a z-length of 250 nm, and a maximum applied force of 200 pN. For each adhesion force map (100 × 100 pixels) from an immune complex spot, 50,000 FD curves were analyzed by JPK data processing software. Adhesion force and stretching distance values were measured by determination of the maximum value for each FD curve.

■ ASSOCIATED CONTENT

Supporting Information

The Supporting Information is available free of charge at https://pubs.acs.org/doi/10.1021/acsomega.2c02009.

Schematic diagram of the etched slide glass; unbinding events for adhesion between captured DISC1 and the detection antibody; observation of the captured-DISC1 cluster; and force maps obtained at three positions in a spot with NDEL1 protein (PDF)

■ AUTHOR INFORMATION

Corresponding Authors

Sang Ki Park − *Department of Life Sciences, Pohang University of Science and Technology, Pohang 37673, Republic of Korea*; Email: skpark@postech.ac.kr

Joon Won Park − *Department of Chemistry, Pohang University of Science and Technology, Pohang 37673, Republic of Korea; Institute of Convergence Science, Yonsei University, Seoul 03722, Republic of Korea*; orcid.org/0000-0003-1432-3161; Email: jwpark@postech.ac.kr

Authors

Donggyu Lee − *Department of Life Sciences, Pohang University of Science and Technology, Pohang 37673, Republic of Korea*

Youngsik Woo − *Department of Life Sciences, Pohang University of Science and Technology, Pohang 37673, Republic of Korea*; orcid.org/0000-0002-8308-8532

Ji-seon Lim − *Department of Chemistry, Pohang University of Science and Technology, Pohang 37673, Republic of Korea*

Ikbum Park − *Analysis and Assessment Research Center, Research Institute of Industrial Science and Technology, Pohang 37673, Republic of Korea*

Complete contact information is available at: https://pubs.acs.org/10.1021/acsomega.2c02009

Notes

The authors declare no competing financial interest.

■ ACKNOWLEDGMENTS

Acknowledges grants from the National Research Foundation of Korea (NRF-2020R1C1C1007055, 2020M3E5E2039894, and 2021R1A2C3010639).

■ REFERENCES

(1) Kim, M.-S.; Pinto, S. M.; Getnet, D.; Nirujogi, R. S.; Manda, S. S.; Chaerkady, R.; Madugundu, A. K.; Kelkar, D. S.; Isserlin, R.; Jain, S.; Thomas, J. K.; Muthusamy, B.; Leal-Rojas, P.; Kumar, P.; Sahasrabuddhe, N. A.; Balakrishnan, L.; Advani, J.; George, B.; Renuse, S.; Selvan, L. D. N.; Patil, A. H.; Nanjappa, V.; Radhakrishnan, A.; Prasad, S.; Subbannayya, T.; Raju, R.; Kumar, M.; Sreenivasamurthy, S. K.; Marimuthu, A.; Sathe, G. J.; Chavan, S.; Datta, K. K.; Subbannayya, Y.; Sahu, A.; Yelamanchi, S. D.; Jayaram, S.; Rajagopalan, P.; Sharma, J.; Murthy, K. R.; Syed, N.; Goel, R.; Khan, A. A.; Ahmad, S.; Dey, G.; Mudgal, K.; Chatterjee, A.; Huang, T.-C.; Zhong, J.; Wu, X.; Shaw, P. G.; Freed, D.; Zahari, M. S.; Mukherjee, K. K.; Shankar, S.; Mahadevan, A.; Lam, H.; Mitchell, C. J.; Shankar, S. K.; Satishchandra, P.; Schroeder, J. T.; Sirdeshmukh, R.; Maitra, A.; Leach, S. D.; Drake, C. G.; Halushka, M. K.; Prasad, T. S. K.; Hruban, R. H.; Kerr, C. L.; Bader, G. D.; Iacobuzio-Donahue, C. A.; Gowda, H.; Pandey, A. A draft map of the human proteome. *Nature* **2014**, *509*, 575−581.

(2) Harper, J. W.; Bennett, E. J. Proteome complexity and the forces that drive proteome imbalance. *Nature* **2016**, *537*, 328−338.
(3) Hanash, S. Disease proteomics. *Nature* **2003**, *422*, 226−232.
(4) Magdeldin, S.; Enany, S.; Yoshida, Y.; Xu, B.; Zhang, Y.; Zureena, Z.; Lokamani, I.; Yaoita, E.; Yamamoto, T. Basics and recent advances of two dimensional- polyacrylamide gel electrophoresis. *Clin. Proteomics* **2014**, *11*, 16.
(5) Telford, W. G.; Hawley, T.; Subach, F.; Verkhusha, V.; Hawley, R. G. Flow cytometry of fluorescent proteins. *Methods* **2012**, *57*, 318−330.
(6) Spitzer, M. H.; Nolan, G. P. Mass cytometry: single cells, many features. *Cell* **2016**, *165*, 780−791.
(7) Junker, J. P.; van Oudenaarden, A. Every cell is special: genome-wide studies add a new dimension to single-cell biology. *Cell* **2014**, *157*, 8−11.
(8) Florin, E.-L.; Moy, V. T.; Gaub, H. E. Adhesion forces between individual ligand-receptor pairs. *Science* **1994**, *264*, 415−417.
(9) Fritz, J.; Katopodis, A. G.; Kolbinger, F.; Anselmetti, D. Force-mediated kinetics of single P-selectin/ligand complexes observed by atomic force microscopy. *Proc. Natl. Acad. Sci. U.S.A.* **1998**, *95*, 12283−12288.
(10) Moy, V. T.; Florin, E.-L.; Gaub, H. E. Intermolecular forces and energies between ligands and receptors. *Science* **1994**, *266*, 257−259.
(11) Rief, M.; Clausen-Schaumann, H.; Gaub, H. E. Sequence-dependent mechanics of single DNA molecules. *Nat. Struct. Mol. Biol.* **1999**, *6*, 346−349.
(12) Strunz, T.; Oroszlan, K.; Schäfer, R.; Güntherodt, H.-J. Dynamic force spectroscopy of single DNA molecules. *Proc. Natl. Acad. Sci. U.S.A.* **1999**, *96*, 11277−11282.
(13) Lee, G. U.; Chrisey, L. A.; Colton, R. J. Direct measurement of the forces between complementary strands of DNA. *Science* **1994**, *266*, 771−773.
(14) Hinterdorfer, P.; Baumgartner, W.; Gruber, H. J.; Schilcher, K.; Schindler, H. Detection and localization of individual antibody-antigen recognition events by atomic force microscopy. *Proc. Natl. Acad. Sci. U.S.A.* **1996**, *93*, 3477−3481.
(15) Allen, S.; Chen, X.; Davies, J.; Davies, M. C.; Dawkes, A. C.; Edwards, J. C.; Roberts, C. J.; Sefton, J.; Tendler, S. J. B.; Williams, P. M. Detection of Antigen−Antibody Binding Events with the Atomic Force Microscope. *Biochemistry* **1997**, *36*, 7457−7463.
(16) Kienberger, F.; Kada, G.; Mueller, H.; Hinterdorfer, P. Single Molecule Studies of Antibody-Antigen Interaction Strength Versus Intra-molecular Antigen Stability. *J. Mol. Biol.* **2005**, *347*, 597−606.
(17) Mori, T.; Sugiyama, S.; Byrne, M.; Johnson, C. H.; Uchihashi, T.; Ando, T. Revealing circadian mechanisms of integration and resilience by visualizing clock proteins working in real time. *Nat. Commun.* **2018**, *9*, 3245.
(18) Rico, F.; Russek, A.; González, L.; Grubmüller, H.; Scheuring, S. Heterogeneous and rate-dependent streptavidin-biotin unbinding revealed by high-speed force spectroscopy and atomistic simulations. *Proc. Natl. Acad. Sci. U.S.A.* **2019**, *116*, 6594−6601.
(19) Husale, S.; Persson, H. H. J.; Sahin, O. DNA nanomechanics allows direct digital detection of complementary DNA and microRNA targets. *Nature* **2009**, *462*, 1075−1078.
(20) Lei, H.; Guo, Y.; Hu, X.; Hu, C.; Hu, X.; Li, H. Reversible unfolding and folding of the metalloprotein ferredoxin revealed by single-molecule atomic force microscopy. *J. Am. Chem. Soc.* **2017**, *139*, 1538−1544.
(21) Dufrêne, Y. F.; Martínez-Martín, D.; Medalsy, I.; Alsteens, D.; Müller, D. J. Multiparametric imaging of biological systems by force-distance curve-based AFM. *Nat. Methods* **2013**, *10*, 847−854.
(22) Lee, Y.; Kim, Y.; Lee, D.; Roy, D.; Park, J. W. Quantification of fewer than ten copies of a DNA biomarker without amplification or labeling. *J. Am. Chem. Soc.* **2016**, *138*, 7075−7081.
(23) Mishra, S.; Lee, Y.; Park, J. W. Direct quantification of trace amounts of a chronic myeloid leukemia biomarker using locked nucleic acid capture probes. *Anal. Chem.* **2018**, *90*, 12824−12831.
(24) Koo, H.; Park, I.; Lee, Y.; Kim, H. J.; Jung, J. H.; Lee, J. H.; Kim, Y.; Kim, J.-H.; Park, J. W. Visualization and quantification of microRNA in a single cell using atomic force microscopy. *J. Am. Chem. Soc.* **2016**, *138*, 11664−11671.
(25) Roy, D.; Kwon, S. H.; Kwak, J.-W.; Park, J. W. "Seeing and Counting" Individual Antigens Captured on a Microarrayed Spot with Force-Based Atomic Force Microscopy. *Anal. Chem.* **2010**, *82*, 5189−5194.
(26) Grüter, R. R.; Vörös, J.; Zambelli, T. FluidFM as a lithography tool in liquid: spatially controlled deposition of fluorescent nanoparticles. *Nanoscale* **2013**, *5*, 1097−1104.
(27) Millar, J. K.; Wilson-Annan, J. C.; Anderson, S.; Christie, S.; Taylor, M. S.; Semple, C. A. M.; Devon, R. S.; Clair, D. M. S.; Muir, W. J.; Blackwood, D. H. R.; Porteous, D. J. Disruption of two novel genes by a translocation co-segregating with schizophrenia. *Hum. Mol. Genet.* **2000**, *9*, 1415−1423.
(28) Mao, Y.; Ge, X.; Frank, C. L.; Madison, J. M.; Koehler, A. N.; Doud, M. K.; Tassa, C.; Berry, E. M.; Soda, T.; Singh, K. K.; Biechele, T.; Petryshen, T. L.; Moon, R. T.; Haggarty, S. J.; Tsai, L.-H. Disrupted in Schizophrenia 1 Regulates Neuronal Progenitor Proliferation via Modulation of GSK3β/β-Catenin Signaling. *Cell* **2009**, *136*, 1017−1031.
(29) Ye, F.; Kang, E.; Yu, C.; Qian, X.; Jacob, F.; Yu, C.; Mao, M.; Poon, R. Y. C.; Kim, J.; Song, H.; Ming, G.-l.; Zhang, M. DISC1 regulates neurogenesis via modulating kinetochore attachment of Ndel1/Nde1 during mitosis. *Neuron* **2017**, *96*, 1041−1054.
(30) Kamiya, A.; Kubo, K.-i.; Tomoda, T.; Takaki, M.; Youn, R.; Ozeki, Y.; Sawamura, N.; Park, U.; Kudo, C.; Okawa, M.; Ross, C. A.; Hatten, M. E.; Nakajima, K.; Sawa, A. A schizophrenia-associated mutation of DISC1 perturbs cerebral cortex development. *Nat. Cell Biol.* **2005**, *7*, 1167−1178.
(31) Young-Pearse, T. L.; Suth, S.; Luth, E. S.; Sawa, A.; Selkoe, D. J. Biochemical and functional interaction of disrupted-in-schizophrenia 1 and amyloid precursor protein regulates neuronal migration during mammalian cortical development. *J. Neurosci.* **2010**, *30*, 10431−10440.
(32) Miyoshi, K.; Honda, A.; Baba, K.; Taniguchi, M.; Oono, K.; Fujita, T.; Kuroda, S.; Katayama, T.; Tohyama, M. Disrupted-In-Schizophrenia 1, a candidate gene for schizophrenia, participates in neurite outgrowth. *Mol. Psychiatr.* **2003**, *8*, 685−694.
(33) Ozeki, Y.; Tomoda, T.; Kleiderlein, J.; Kamiya, A.; Bord, L.; Fujii, K.; Okawa, M.; Yamada, N.; Hatten, M. E.; Snyder, S. H.; Ross, C. A.; Sawa, A. Disrupted-in-Schizophrenia-1 (DISC-1): mutant truncation prevents binding to NudE-like (NUDEL) and inhibits neurite outgrowth. *Proc. Natl. Acad. Sci. U.S.A.* **2003**, *100*, 289−294.
(34) Hayashi-Takagi, A.; Takaki, M.; Graziane, N.; Seshadri, S.; Murdoch, H.; Dunlop, A. J.; Makino, Y.; Seshadri, A. J.; Ishizuka, K.; Srivastava, D. P.; Xie, Z.; Baraban, J. M.; Houslay, M. D.; Tomoda, T.; Brandon, N. J.; Kamiya, A.; Yan, Z.; Penzes, P.; Sawa, A. Disrupted-in-Schizophrenia 1 (DISC1) regulates spines of the glutamate synapse via Rac1. *Nat. Neurosci.* **2010**, *13*, 327−332.
(35) Duan, X.; Chang, J. H.; Ge, S.; Faulkner, R L.; Kim, J. Y.; Kitabatake, Y.; Liu, X. B.; Yang, C. H.; Jordan, J. D.; Ma, D. K.; Liu, C. Y.; Ganesan, S.; Cheng, H. J.; Ming, G. L.; Lu, B.; Song, H. Disrupted-In-Schizophrenia 1 regulates integration of newly generated neurons in the adult brain. *Cell* **2007**, *130*, 1146−1158.
(36) Kim, J. Y.; Duan, X.; Liu, C. Y.; Jang, M.-H.; Guo, J. U.; Pow-anpongkul, N.; Kang, E.; Song, H.; Ming, G.-l. DISC1 regulates new neuron development in the adult brain via modulation of AKT-mTOR signaling through KIAA1212. *Neuron* **2009**, *63*, 761−773.
(37) Taya, S.; Shinoda, T.; Tsuboi, D.; Asaki, J.; Nagai, K.; Hikita, T.; Kuroda, S.; Kuroda, K.; Shimizu, M.; Hirotsune, S.; Iwamatsu, A.; Kaibuchi, K. DISC1 Regulates the Transport of the NUDEL/LIS1/14-3-3 Complex through Kinesin-1. *J. Neurosci.* **2007**, *27*, 15−26.
(38) Millar, J. K.; Pickard, B. S.; Mackie, S.; James, R.; Christie, S.; Buchanan, S. R.; Malloy, M. P.; Chubb, J. E.; Huston, E.; Baillie, G. S.; Thomson, P. A.; Hill, E. V.; Brandon, N. J.; Rain, J.-C.; Camargo, L. M.; Whiting, P. J.; Houslay, M. D.; Blackwood, D. H. R.; Muir, W. J.; Porteous, D. J. DISC1 and PDE4B are interacting genetic factors in schizophrenia that regulate cAMP signaling. *Science* **2005**, *310*, 1187−1191.

https://doi.org/10.1021/acsomega.2c02009
ACS Omega 2022, 7, 20165−20171

(39) Sawamura, N.; Ando, T.; Maruyama, Y.; Fujimuro, M.; Mochizuki, H.; Honjo, K.; Shimoda, M.; Toda, H.; Sawamura-Yamamoto, T.; Makuch, L. A.; Hayashi, A.; Ishizuka, K.; Cascella, N. G.; Kamiya, A.; Ishida, N.; Tomoda, T.; Hai, T.; Furukubo-Tokunaga, K.; Sawa, A. Nuclear DISC1 regulates CRE-mediated gene transcription and sleep homeostasis in the fruit fly. *Mol. Psychiatr.* **2008**, *13*, 1138−1148.
(40) Soda, T.; Frank, C.; Ishizuka, K.; Baccarella, A.; Park, Y.-U.; Flood, Z.; Park, S. K.; Sawa, A.; Tsai, L.-H. DISC1-ATF4 transcriptional repression complex: dual regulation of the cAMP-PDE4 cascade by DISC1. *Mol. Psychiatr.* **2013**, *18*, 898−908.
(41) Ogawa, F.; Malavasi, E. L. V.; Crummie, D. K.; Eykelenboom, J. E.; Soares, D. C.; Mackie, S.; Porteous, D. J.; Millar, J. K. DISC1 complexes with TRAK1 and Miro1 to modulate anterograde axonal mitochondrial trafficking. *Hum. Mol. Genet.* **2014**, *23*, 906−919.
(42) Park, C.; Lee, S.-A.; Hong, J.-H.; Suh, Y.; Park, S. J.; Suh, B. K.; Woo, Y.; Choi, J.; Huh, J.-W.; Kim, Y.-M.; Park, S. K. Disrupted-in-schizophrenia 1 (DISC1) and Syntaphilin collaborate to modulate axonal mitochondrial anchoring. *Mol. Brain* **2016**, *9*, 69.
(43) Park, S. J.; Lee, S. B.; Suh, Y.; Kim, S.-J.; Lee, N.; Hong, J.-H.; Park, C.; Woo, Y.; Ishizuka, K.; Kim, J.-H.; Berggren, P.-O.; Sawa, A.; Park, S. K. DISC1 Modulates Neuronal Stress Responses by Gate-Keeping ER-Mitochondria Ca 2+ Transfer through the MAM. *Cell Rep.* **2017**, *21*, 2748−2759.
(44) Park, Y.-U.; Jeong, J.; Lee, H.; Mun, J. Y.; Kim, J.-H.; Lee, J. S.; Nguyen, M. D.; Han, S. S.; Suh, P.-G.; Park, S. K. Disrupted-in-schizophrenia 1 (DISC1) plays essential roles in mitochondria in collaboration with Mitofilin. *Proc. Natl. Acad. Sci. U.S.A.* **2010**, *107*, 17785−17790.
(45) Hong, B. J.; Oh, S. J.; Youn, T. O.; Kwon, S. H.; Park, J. W. Nanoscale-controlled spacing provides DNA microarrays with the SNP discrimination efficiency in solution phase. *Langmuir* **2005**, *21*, 4257−4261.
(46) Schneider, C.; Newman, R. A.; Sutherland, D. R.; Asser, U.; Greaves, M. F. A one-step purification of membrane proteins using a high efficiency immunomatrix. *J. Biol. Chem.* **1982**, *257*, 10766−10769.
(47) Lee, Y.; Kwon, S. H.; Kim, Y.; Lee, J.-B.; Park, J. W. Mapping of surface-immobilized DNA with force-based atomic force microscopy. *Anal. Chem.* **2013**, *85*, 4045−4050.
(48) Brummelkamp, T. R.; Bernards, R.; Agami, R. A system for stable expression of short interfering RNAs in mammalian cells. *Science* **2002**, *296*, 550−553.
(49) Park, S. J.; Jeong, J.; Park, Y.-U.; Park, K.-S.; Lee, H.; Lee, N.; Kim, S.-M.; Kuroda, K.; Nguyen, M. D.; Kaibuchi, K.; Park, S. K. Disrupted-in-schizophrenia-1 (DISC1) regulates endoplasmic reticulum calcium dynamics. *Sci. Rep.* **2015**, *5*, 8694.

https://doi.org/10.1021/acsomega.2c02009
ACS Omega 2022, 7, 20165−20171